Sedimentology (1980) **27**, 31–46

A physical model for the transport and sorting of fine-grained sediment by turbidity currents

DORRIK A. V. STOW* & ANTHONY J. BOWEN

Departments of Geology and Oceanography, Dalhousie University, Halifax, N.S., Canada

ABSTRACT

Turbidite muds in cores from the outer Scotian continental margin, off eastern Canada, contain abundant thin silt laminae. Graded laminated units are recognized in parts of this sequence. These represent single depositional events, and show a regular decrease in modal grain size and thickness of the silt laminae through the unit. A similar fining trend is shown by both silt and mud layers over hundreds of kilometres downslope. Textural analysis of individual laminae allows the construction of a dynamically consistent physical model for transport and sorting in muddy turbidity currents. Hydraulic sorting aggregates finer material to the top and tail regions of a large turbidity flow which then overspills its channel banks. Downslope lateral sorting occurs with preferential deposition of coarser silt grains and larger mud flocs. Depositional sorting by increased shear in the boundary layer separates clay flocs from silt grains and results in a regular mud/silt lamination. Estimates can be made of the physical parameters of the turbidity flows involved. They are a minimum of several hundreds of metres thick, have low concentrations (of the order of 10^{-3} or 2500 mg l^{-1}), and move downslope at velocities of 10–20 cm s^{-1}. A 5 mm thick, coarse silt lamina takes about 10 h to deposit, and the subsequent mud layer 'blankets' very rapidly over this. A complete unit is deposited in 2–6 days which is the time it takes for the turbidity flow to pass a particular point. These thick, dilute, low-velocity flows are significantly different from the 'classical' turbidity current. However, there is mounting evidence in support of the new concept from laboratory observations and direct field measurements.

INTRODUCTION

Fine-grained sediments (clays and silts) make up much of the fill of ocean basins and the modern cover of coastal and shelf environments. However, less attention has been paid to the process of transport and deposition of this material than to the volumetrically less important sands and gravels (McCave, 1972; Piper, 1978). A variety of mechanisms has been proposed for the transport of fine sediment into deep water. They include, the settling of pelagic, hemipelagic and ice rafted material (Davies & Laughton, 1972); deposition from nepheloid layers (Ewing & Thorndike, 1965; Ewing *et al.*, 1971); deposition from bottom currents (Heezen, Hollister & Ruddiman, 1966; Hollister, 1967); and deposition from large-scale turbidity currents (Hesse, 1975; Piper, 1978). Various low-velocity, low-density flows have also been proposed (Gorsline, Drake & Barnes, 1968; Moore, 1969; McCave, 1972; Shepard *et al.*, 1977).

Textural analyses of late Wisconsin muds and silts on the outer continental margin off Nova Scotia reveal pronounced downslope trends in grain size parameters (Stow, 1976, 1977). These sediments have been shown to be mostly turbidites (Stow, 1979) and probably result from relatively slow, widespread 'sheet' flows caused by large turbidity currents overtopping their channel levees.

* Present address: British National Oil Corporation, 150 St Vincent Street, Glasgow, Scotland

0037-0746/80/0200-0031 $02.00

A physical model is developed in this paper to explain the observed sorting, to derive general estimates of the flow parameters (Fig. 1), and to attempt an explanation of the silt/mud lamination.

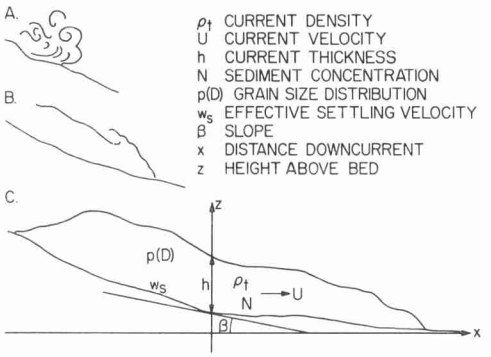

Fig. 1. Development of a fine-grained turbidity current from a slump, and definition of current parameters.

OBSERVATION

The late Quaternary geology of the deep water margin off Nova Scotia (Fig. 2) has been discussed by Piper (1975) and Stow (1975, 1977, 1979). During periods of lowered sea-level much of the wide continental shelf was exposed. A floating ice shelf probably existed in the Laurentian Channel and large amounts of sediment were supplied to the upper slope. Slumping of this material resulted in its downslope transport via turbidity currents. Coarse sands and gravels were deposited in deeply incised channels while the fine-grained sediment built up thick inter-channel deposits over the Laurentian Fan and adjacent slope and rise. Smaller turbidity currents were also initiated in the heads of submarine canyons along the shelf-break shore edge. Reworking of more slowly deposited hemipelagic sediments by the contour following Western Boundary Undercurrent was only significant during interstadial periods and the Holocene.

More than fifty cores and many hundreds of silt, sand and mud layers have been examined for the present study using visual descriptive and X-radiographic techniques. Over 200 size analyses have been carried out using the pipette and sieve method (Laughton, Berggren *et al.*, 1972), and a model T Coulter Counter (Sheldon & Parsons, 1967).

The silt laminae vary in thickness between <0·5 and 10 mm. The thicker ones commonly have sharp bases and sharp or gradational tops; the thinner ones are less clearly defined. They occur either as distinct graded laminated units (Piper, 1972) between 1 and 10 cm thick (Fig. 3), or as continuous silt laminated sequences. Size analyses of grouped silt laminae are shown in Fig. 4. There may be several prominent silt laminae showing a slight decrease in modal size through the unit; or one distinct, coarser basal lamina overlain by numerous thinner, finer laminae (Fig. 4). The intercalated muds are less clearly graded. Total size analysis through a single unit (either by proportional summation of separate analyses or by channel sampling) reveals an even distribution spanning a wide range of grain sizes (Fig. 4). Mineralogical and structural evidence suggests that these graded laminated units were deposited as single sedimentation events (Stow, 1977).

A similar fining trend is apparent from size analyses of the more prominent (basal) laminae from slope through rise to abyssal plain environments over a distance greater than 1000 km (Fig. 5a). The decrease in modal size with distance downslope is still more pronounced in the interlaminated muds (Fig. 5b). A plot of standard deviation versus mean size emphasizes the trend in sorting of the fine silt laminae (Fig. 6). Mean size generally decreases downslope and away from channel axes. The finer, more 'distal' laminae are less well sorted. This is in contrast to Piper's (1978) model which suggests a slow process of segregation of silt from clay flocs during turbidity current transport and, hence, improved sorting in the direction of transport.

SEDIMENTATION

Clayey sediment flocculates readily in sea water. The most important factors controlling this flocculation are the concentration of particles within the suspending fluid (Migniot, 1971) and the turbulence intensity (Krone, 1959, 1962; Einstein & Krone, 1961; Partheniades, 1965). Over a period of time, continued flocculation results in progressively larger clay–water aggregates with greater settling velocities and lower densities and shear strengths (Krone, 1963; Moon, 1972). According to Partheniades (1965) these floc aggregates will reach a maximum equilibrium diameter related to the turbulence intensity. Kranck (1973) believes that the stable floc size distributions obtained in sea water are determined primarily by the initial size of the individual grains. The floc mode is always larger than

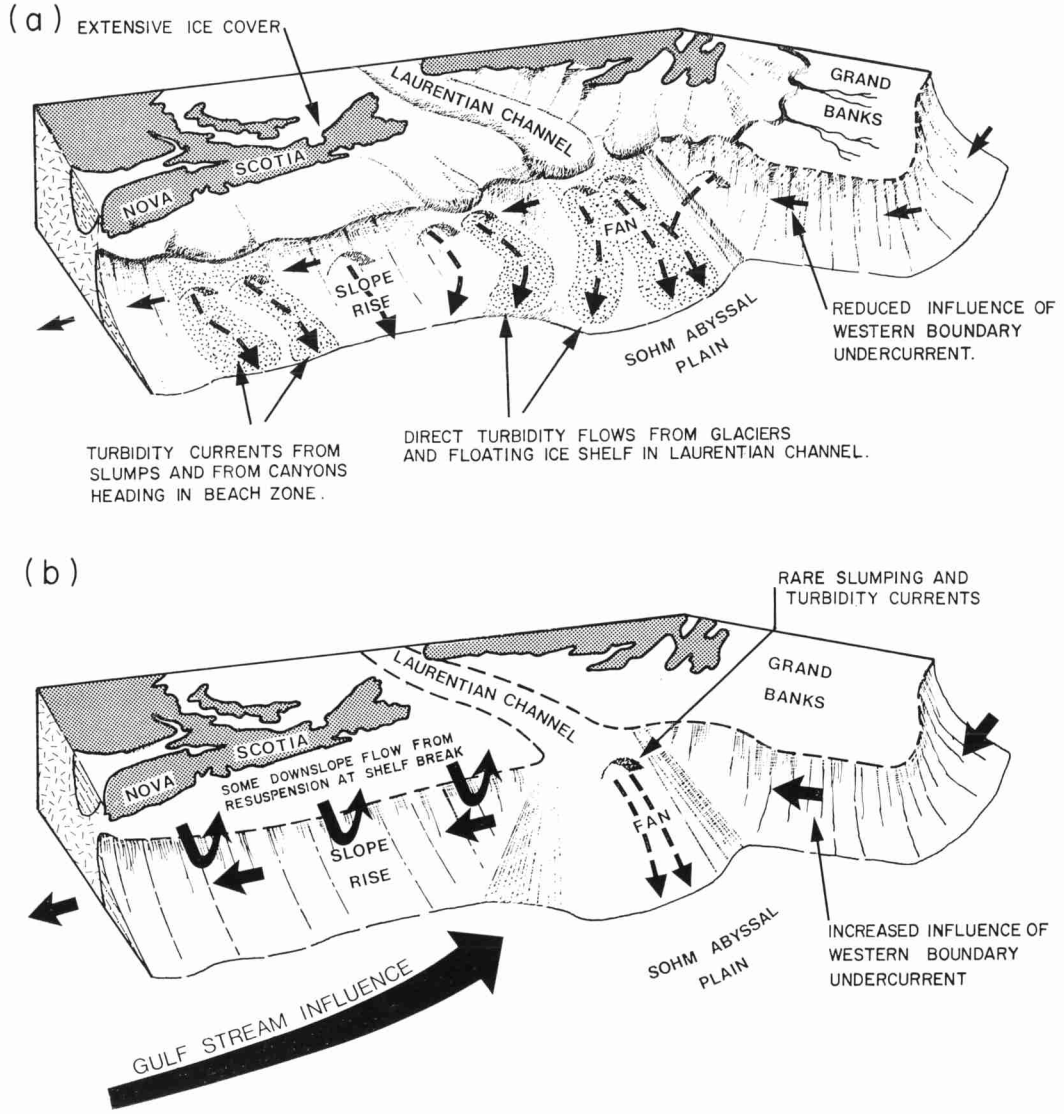

Fig. 2. Summary of sedimentation on Nova Scotian outer continental margin during glacial and non-glacial periods (a) Glaciated margin, Wisconsin; (b) non-glaciated margin, Holocene.

the original grain mode, and the floc settling velocity is probably of the same order as that for the largest individual grains present in a suspension (Whitehouse, Jeffrey & Debbrecht, 1960; Partheniades, Cross & Ayora, 1969; Kranck, 1973).

Deposition of fine-grained sediment occurs when flocs form strong enough bonds to resist the flow-induced, disruptive shear stress near the bed (Partheniades *et al.*, 1969). There appears to be a critical velocity above which fine sediment does not deposit. Values ranging from 15 to 25 cm s^{-1} have been given by Einstein & Krone (1962), Krone (1962), Partheniades (1965) and Partheniades *et al.* (1969). Other work on the deposition of fine sediment is summarized by Partheniades (1964), Odd & Owen (1972), Krone (1972, 1976), Buller, Green & McManus (1975) and McCave (1970, 1972, 1976). According to these authors, the most important factors controlling deposition are: flow turbulence, bed shear stress, and the concentration and settling

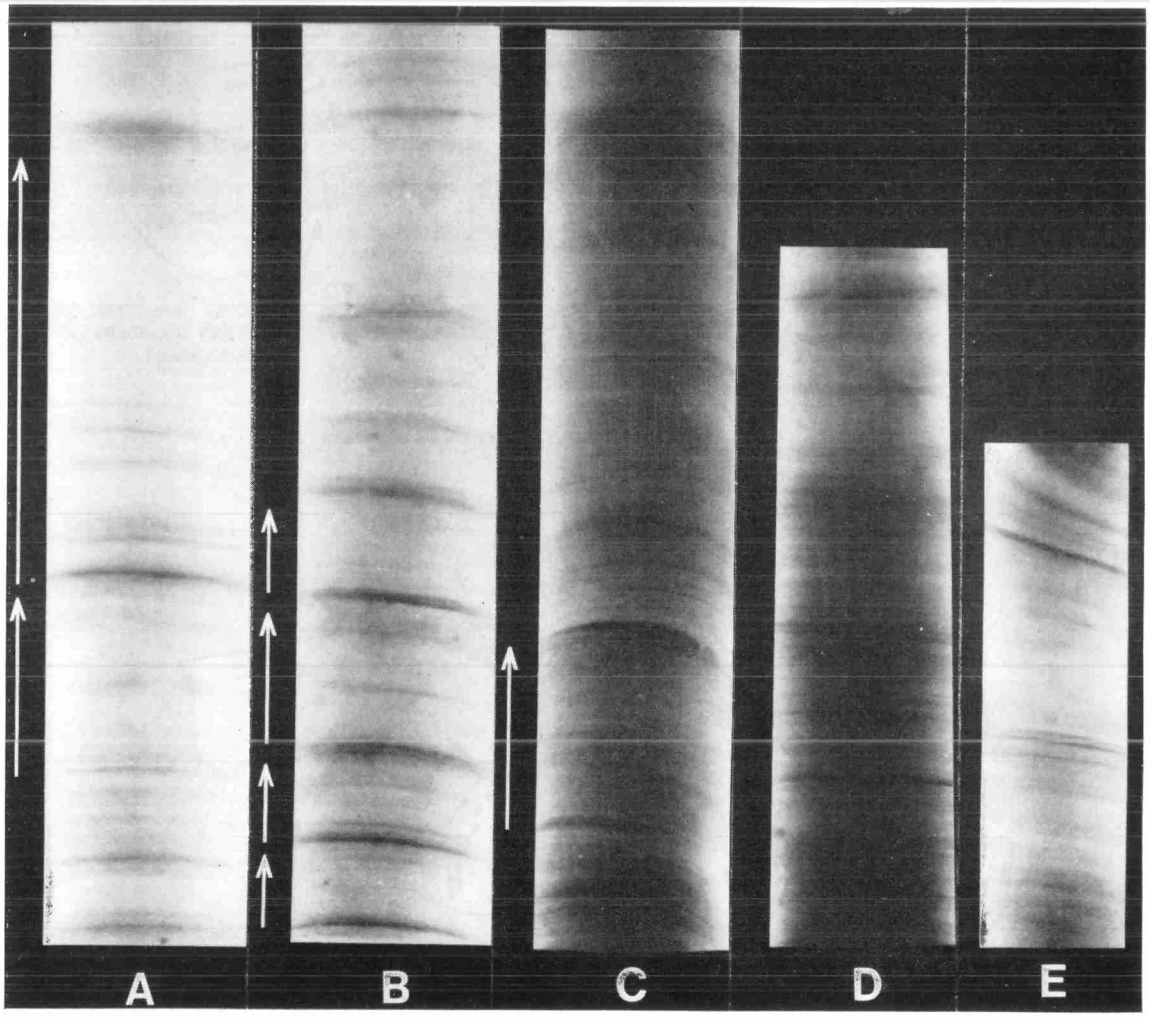

Fig. 3. X-radiograph positives of laminated mud facies in Scotian margin cores. Typical, graded laminated units are indicated by the arrows in A, B and C. In D and E these units are less clearly recognized. The width of the core sections is about 4 cm.

velocity of the sediment. More minor controls are the sediment properties and composition (silt and clay behave very differently), water chemistry, and the nature of the depositional surface.

Further information on the behaviour of fine sediment may be derived from studies of erosion (Partheniades & Paaswell, 1968; Migniot, 1968; Einsele *et al.*, 1974; Young & Southard, 1978). The most important factors affecting the critical erosion stress for muddy sediments are the sediment nature (clay type, bulk density, consolidation, etc.), the bottom topography and the bed shear stress. White (1970) investigated the plane bed thresholds of fine-grained, non-cohesive sediments. He found that the absolute value of stress for erosion decreases slowly as the size decreases below 200 μm (see also data of Miller, McCave & Komar, 1977).

CALCULATIONS

Rate of deposition

Although the bulk properties of a turbidity current may be described by an overall concentration N and

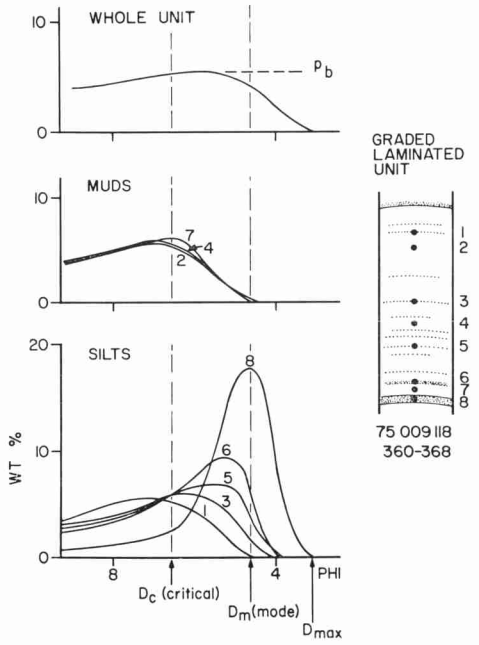

Fig. 4. Smoothed, weight %, grain-size curves from analyses of individual silt layers, mud layers and the whole graded laminated unit shown as a schematic core section on the right. The numbers beneath the core section are the core code and section depth in cm. The critical grain diameter (D_c), silt mode (D_m) and maximum silt size (D_{max}) are shown. See text for further discussion.

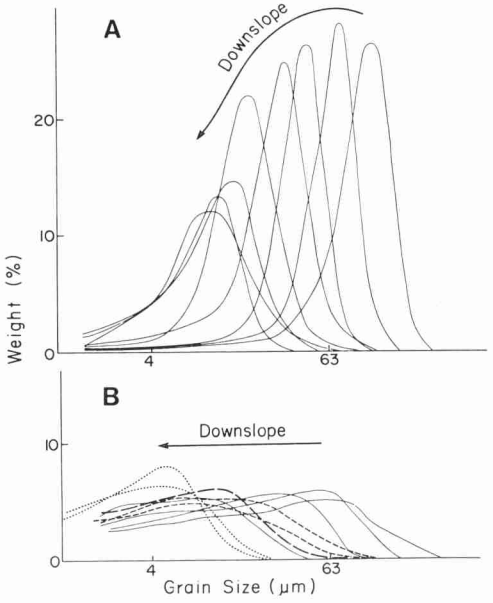

Fig. 5. Downslope textural trends in silts (A) and muds (B) from Scotian margin cores. The distance between samples is of the order of 100 km.

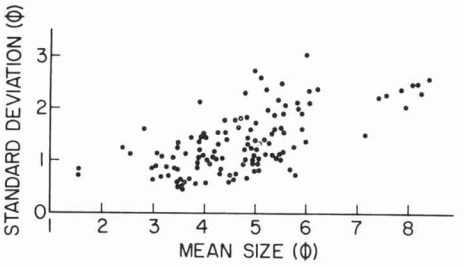

Fig. 6. Standard deviation versus mean size for Scotian margin and Sohm Abyssal Plain thin sands and silts. The mean size also decreases with distance offshore so that sorting becomes poorer (i.e. standard deviation increases) downslope.

a typical settling velocity w_s (Fig. 1), any detailed calculation requires further insight into the distribution of particle size and composition.

McCave & Swift (1976) have suggested that the rate of deposition, R of sediment of settling velocity w, is given by an equation of the form,

$$R = \rho_s C w P \qquad (1)$$

where C is the concentration of the sediment of settling velocity, w and density, ρ_s, in the flow just above the viscous sublayer of the bottom boundary layer (note that N, above, is the concentration of *all* grain sizes in the *entire* flow); and P is the probability that a given particle will be deposited. Data from experiments with fine, non-cohesive silt (White, 1970), lead to the suggestion that P is given by

$$P = p'\left[1 - \frac{\tau}{\tau_c(w)}\right] \qquad (2)$$

where τ is the local bottom stress, $\tau_c(w)$ a critical value for the deposition of sediment of settling velocity w, and p' is a factor to account for other influences on the probability of deposition. McCave & Swift (1976) give a plot of τ_c as a function of w, based largely on the data of White (1970). This is generally in line with experiments on the deposition of cohesive material, discussed earlier.

For muds, there is no simple relationship between the grain size obtained by analysis of the deposit, and the dynamic behaviour of flocculated particles in suspension. The relationship between grain-size distribution and particle-size distribution has been discussed by Kranck (1973, 1975).

In the case of silts behaving as individual particles, the settling velocity w is a well defined function of the

grain diameter and density. Equations 1 and 2 can be rewritten as

$$R(D)=\rho_s\ C(D)\ w(D)\ p'\left[1-\frac{\tau}{\tau_c(D)}\right] \qquad (3)$$

for grain diameter D. Any layer deposited in time T_0 will be made up of contributions from the various sediment sizes (of differing settling velocities) in suspension. If a layer of thickness q is identified in a core, sediment analysis provides both the bulk density (volume concentration) of the deposited sediment N_s and the proportion of each size component, the grain-size distribution $p_s(D)$.

This was deposited over some unknown period of time T_0, where, for any particular size

$$p_s(D)N_s q\rho_s=R(D)T_0 \qquad (4)$$

and for the whole layer

$$\rho_s q N_s=T_0 \sum_D R(D). \qquad (5)$$

From Equations 3 and 4, since $\Sigma\, p_s(D)=1$

$$p_s(D)=\frac{C(D)w(D)}{Q}\left[1-\frac{\tau}{\tau_c(D)}\right] \qquad (6)$$

where

$$Q=qN_s/p'T_0$$

and $C(D)$ can be re-expressed as $P_b(D)N_b$ where N_b is the total sediment concentration and $p_b(D)$ the grain-size distribution in the flow just above the viscous sublayer.

Inferences from silt and mud laminae

There are three unknown quantities in Equation 6 : Q, τ and C. p_s, w and τ_c are known or measured functions of grain size provided the sediment behaves dynamically as individual grains. Of the unknowns, $C(D)$ is a function of grain size, representing the distribution of grain sizes in the flow just above the viscous sublayer, τ is a property of the flow independent of grain size, Q is a collection of parameters of which q and N_s can be measured, T_0 is unknown, and p' might be a function of grain size. Clearly the values of τ, T_0 and p' are of great interest. Can they be estimated?

An important consequence of Equations 3 and 6 is that there should be no material deposited of grain size less than some critical diameter, D_c, given by

$$\tau=\tau_c(D_c) \qquad (7)$$

Inspection of the size distribution of the silty layers in Scotian margin sediments shows a small quantity of very fine material, but a distinct change in trend at some intermediate grain size (Fig. 4). This provides a first, crude estimate of D_c and hence, using McCave & Swift (1976), of the actual stress, τ, at the time of deposition. Implicit in the above assumptions is that there are finer particles in the flow not being deposited because τ is too large.

Figure 4 represents typical size analyses of silt laminae and superjacent mud layers. Inspection of the size distribution of the superjacent mud layers shows that the coarse tail begins to fall off at the same size interval that the silt curve changes to a marked upward trend. This point, therefore, also provides a crude estimate of τ_c. The curve decreases to zero at a grain size close to that of the modal silt (Fig. 4). This close match between silt and superjacent mud is, clearly, strong evidence that they were deposited almost simultaneously from the same flow. The flow is one in which grains are behaving as individual silt particles during the depositional phase. Proportional summation of these analyses, or measurement of a continuous sample through the couplet, shows a fairly even distribution of grain sizes for the 'silt + mud couplet', in the size ranges below the median silt size.

The size distribution of the couplet provides an estimate of the size distribution of the suspension from which first the silt and then the mud are deposited (Stow & Bowen, 1978). $C(D)$ may be approximately constant for the sizes between D_{mode} and D_c or less (Fig. 4). This can be checked by using Equation 6 for the distribution of the silt layer, grain size by grain size. For any particular size D_0,

$$\frac{Q}{C}=\frac{w(D_0)}{p_s(D_0)}\left[1-\frac{\tau}{\tau_c(D_0)}\right] \qquad (8)$$

giving a line on a plot of Q/C *vs* τ (Fig. 7) for each grain size. As can be seen in Fig. 7, the data for a number of grain sizes lead to a set of equations that are all satisfied by a particular value of τ and Q/C, given by the point of intersection of the lines. This provides an estimate of actual bottom stress at the

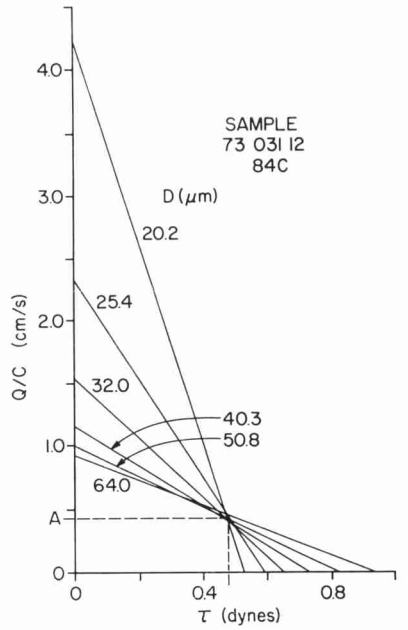

Fig. 7. Estimate of critical shear stress (τ_c) from the modal size distribution of a particular silt lamina. Using Equation 4 Q/C is plotted against τ for each grain size interval (D); the confluence of lines give τ_c and A (a particular value of Q/C).

time of deposition. Of course, this gives roughly the same result as looking for τ_c in either the silt or mud size distributions. Equally significantly, it suggests Q/C is not a function of grain size (if it were the lines in Fig. 7 would not converge to a single point).

The simplest assumption from the evidence of the silt deposition and the knowledge of the properties of the silt + mud couplet is that neither $C(D)$ nor p' are strong functions of grain size. An even distribution of grain sizes in the boundary layer (Fig. 8) is made up of a coarse silt mode and a fine mud tail. The coarse silt settles into the boundary layer as individual grains, while the mud probably settles as flocs where,

$$D_{\text{mode (flocs)}} > D_{\text{mode (silt)}}$$

and the effective floc settling velocity is of the same order as that of the silt. The finest silt and the smaller flocs are left behind in the turbidity current.

Model for depositional sorting

Within a fine-grained turbidity current there will be clay flocs and silt grains having equivalent settling velocities, so that the expected deposit from a waning current would be a graded, silty-mud. In most cases, however, the depositional unit is distinctly laminated as well as graded. Such silt-laminated muds are a very common deep marine facies and occur repeatedly in the geological record. A variety of mechanisms has been proposed for their origin. These include: current pulsations (Lombard, 1963; Sanders, 1960, 1965; Lambert, Kelts & Marshall, 1976); multiple events (Kingma, 1958; Wood & Smith, 1959; Moore, 1969); congregational sorting (Kuenen, 1966; Piper, 1972) migration of bed forms (Jopling, 1964, 1966, 1967); and reworking by bottom currents (Hollister, 1967). A more complete review is given in Stow (1977). The separation of mud and silt layers in outer Scotian margin sediments is believed to be primarily due to depositional sorting in the boundary layer at the base of a turbidity current (Fig. 8).

The sediment concentration gradients within the turbidity current are maintained by turbulent mixing, such that the sediment concentration for a particular size fraction pN, in the flow is less than that just above the boundary layer p_0N_b; the ratio p_0/p being largest for large diameter particles (Hjulstrom, 1939). However, for small particles ($w \sim 10^{-2}$ cm s^{-1}) McCave (1970) has shown that the downward

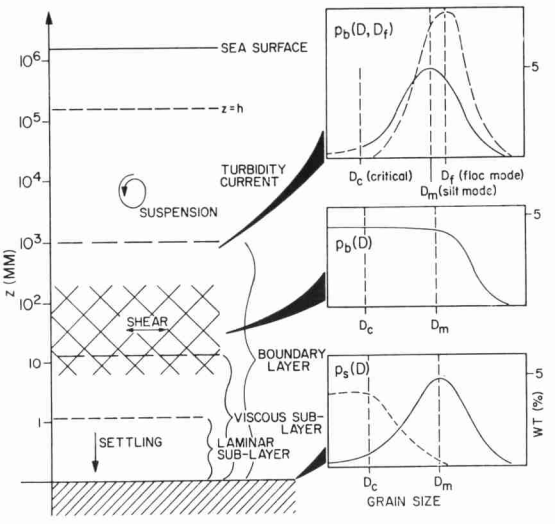

Fig. 8. Model for shear sorting in the boundary layer of a turbidity current. Depth measured from sea floor in a millimetre logarithmic scale. The boxes on the right show the probable grain-size distributions at different levels within the boundary layer and the measured grain-size distribution of the sediment.

increase in concentration is small for reasonable mixing values. As a first approximation then, we may take,

$$p=p_0,\ N=N_b$$

for either clay flocs (diameter, D_f) or silt grains (diameter, D). As the particles fall towards the bed the increased shear in the boundary layer causes the clay floes to break up (Krone, 1962; Partheniades *et al.*, 1969). Initially N_b remains constant, while the size distribution p_0 changes due to deflocculation to a new distribution p_b more nearly representing the distribution of solid particles (Fig. 8).

$$p_0(D_f,\ D)\rightarrow p_b(D)$$

The silt grains settle through the viscous sublayer to form a silt lamina (Fig. 9a and b). As more sediment is supplied to the top of the boundary layer the mud concentration builds up, and some reflocculation may occur (Fig. 9c). At some critical concentration the clays are able to form sufficiently large aggregates that they overcome shear, break-up and deposit rapidly through the laminar sublayer as a mud 'blanket' over the coarser silt lamina (Fig. 9d). The cycle of silt and mud deposition is then repeated for successively finer grain sizes.

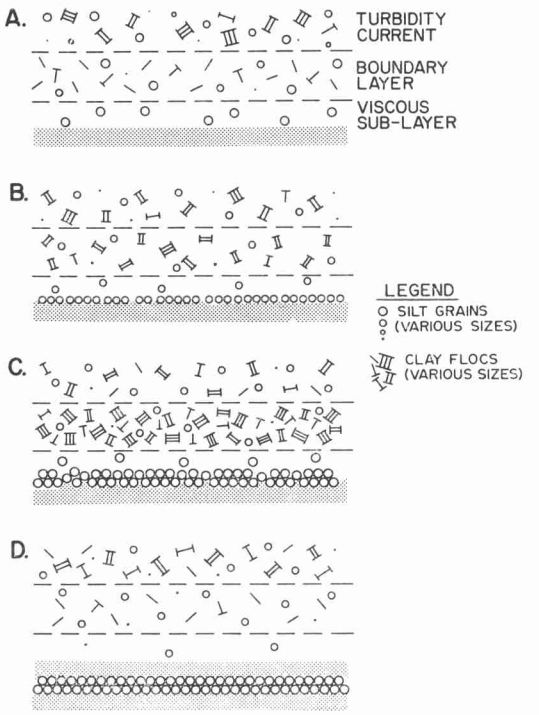

Fig. 9. Schematic representation of the stages of silt and mud deposition through the boundary layer of a turbidity current to form silt and mud laminae.

While separation of mud and silt in this way does appear to be a necessary corollary of boundary layer shear, it is not clear why the mud deposits so rapidly. Temporary disturbance of the boundary layer structure (by velocity fluctuations, etc.), or the partial development of a cohesive bed surface as the largest flocs manage to settle through the sublayer, are possible explanations. The increased mud concentration may affect these processes (Einstein & Krone, 1962) or may be sufficient alone to cause mud blanketing. Experimental work with mud slurries does suggest that they deposit more rapidly with increasing concentration (Migniot, 1968). The fact that the mud does deposit very rapidly is indicated by the absence of coarse silt particles from the mud layer.

This model suggests that coarse silt layers should generally be thicker than the subsequent fine silt layers. As the coarser silts have a higher settling velocity, proportionately more coarse silt should be deposited before the concentration of mud in the viscous sublayer becomes 'critical'. At lower settling velocities the silt layers should become finer and thinner, and there will be a higher proportion of mud relative to silt. Apart from the effects arising from the general slowing of the current, the mud layers should be of rather constant thickness.

The graded, laminated units clearly show the expected trends (Fig. 4). There is even a general correlation between layer thickness and modal silt size for all cores (Fig. 10). However, the modal size is also roughly correlated with the current velocity (Table 1), which could also be a factor in determining layer thickness.

General equations for a turbidity current

In order to test the validity of the deposition model, and also to infer total flow characteristics, we can look at the dynamic constraints on the turbidity current itself.

The stability of the upper surface of a turbidity current has been discussed by Ippen & Harleman (1952) and Harleman (1961) who define the densimetric Froude Number,

$$Fr=\frac{U}{[(\rho_t-\rho)gh/\rho_t)^{\frac{1}{2}}} \qquad (9)$$

Table 1. Details of sediment samples and estimates of turbidity current parameters

Sample	Distance from shelf break (x km)	Bottom slope ($\tan\beta$)	Lamina thickness (q mm)	Modal grain size (D_m μm)	Settling velocity [$W(D_m)$ cms^{-1}]	Critical shear stress Q/C (dynes) (A cm s^{-1})			Flow velocity (U cm s^{-1})	($U\tan\beta$ cm s^{-1})	Flow thickness (m) $\left(\frac{p'x}{h}\right)$	$\left(\frac{h}{p'}\right)$	Time for lamina deposition, (T_0 hours) for flow concentrations:		
						first estimate	graphical estimate	graphical estimate					$N_b=10^{-4}$	10^{-3}	10^{-2}
1	110	0·015	6	84·6	0·35	0·42	0·48	0·42	14	0·210	75	1500	100	10	1
2	110	0·015		(50·8)		0·37									
3	110	0·015		(84·6)		0·47									
4	270	0·005	4	32·0	0·05		0·32		11	0·055	435	620	70	7	0·7
5	230	0·005	1	32·0	0·05		0·29	0·09	11	0·055	400	580	140	14	1·4
6	230	0·005		32·0											
7	230	0·005	2	40·3	0·08	0·33	0·35	0·11	12	0·060	285	800			
8	230	0·005	2	32/40·3											
9	230	0·005	1	32·0											
10	230	0·005	1·5	32·0	0·05		0·19	0·11	9	0·045	255	900	95	9·5	1
11	230	0·005	1·5	32/40·3	0·065	0·26	0·20	0·12	9	0·045	200	1150	90	9	0·9
12	230	0·005	4	40·3/50·8	0·10	0·33	0·35	0·15	12	0·060	200	1150			
13	240	0·009	11	40·3/50·8	0·10	0·29	0·26	0·19	10	0·090	140	1700	385	38·5	4
14	240	0·009		50·8		0·47									
15	75	0·030		128		0·47									
16	75	0·030		(128)		0·53									
17	75	0·030	6	101·6/128	0·61		0·48	1·0	14	0·420	60	1250	42	4·2	0·4
18	75	0·030		(128)		0·47									
19	270	0·005	9	64	0·20	0·42	0·38	0·80	12·5	0·063	105	2600	90	9	0·9
20	270	0·005		(50·8)		0·37									
21	115	0·012	2	40·3	0·081	0·33	0·29	0·10	11	0·132	225	510	140	14	1·4
22	115	0·012		(50·8)	(0·13)	0·33				(0·132)	(130)	(880)			
23	30	0·040		84·6	0·35		0·55	0·80	15·5	0·62	95	320			
24	150	0·015	20	84·6	0·35	0·55	0·60	0·40	16	0·24	105	1450	350	35	3·5
25	500	0·001		50·8/64·0	0·16	0·42			13	0·013	165	3000			
26	990	0·0003		10·08	0·0053				12	0·0036	2000	500			
27	1450	0·0003		6·35/8·00	$6{\cdot}5{\cdot}10^{4}$				12	0·0036	2500	600			

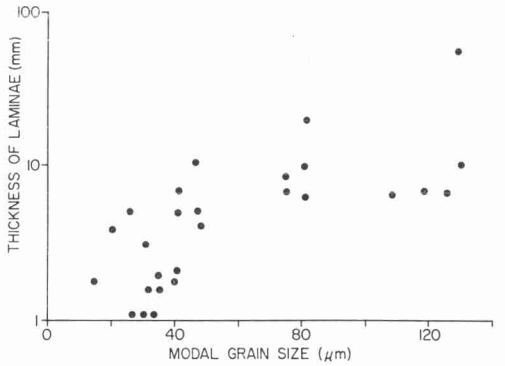

Fig. 10. Coarse layer thickness versus modal grain size for Scotian margin sands and silts. The trend of increasing layer thickness with increasing grain size is predicted by the proposed model for depositional sorting.

where ρ_t is the mean density of the current, ρ is the fluid density, h is the depth of the current, and U the mean velocity.

Bagnold (1962) has shown that the equation for the flow of a turbidity current can be expressed as,

$$(\rho_t - \rho)\, gh(U \sin \beta - \bar{w} \cos \beta) = \tau U \qquad (10)$$

where β is the bottom slope. The effective settling velocity $\bar{w}$ of the suspension is given by

$$\bar{w} = \frac{\Sigma\, pw}{\Sigma\, p} \qquad (11)$$

where p is the proportion of the grain-size distribution in suspension with settling velocity w (Bagnold, 1956).

Equation 10 reduces to the Chezy equation frequently used to describe turbidity currents (Komar, 1971, 1973), if $w \ll U \tan \beta$. The bottom stress can be expressed as,

$$\tau = \rho U^2_* = \rho c_f U^2 \qquad (12)$$

where c_f is a dimensionless drag coefficient, and U_* is the friction velocity. Values of c_f can be estimated from McCave (1970) or Daily & Harleman (1966) following Komar (1970). Typical values are in the range 2×10^{-3} to 3×10^{-3}, not a significant variation in terms of the present study. Combining Equations 9, 10 and 12 the Froude Number can be expressed as,

$$Fr = \left[\frac{\sin \beta}{c_f} \left(1 - \frac{w}{U \tan \beta}\right) \right]^{\frac{1}{2}} \qquad (13)$$

For reasonable values of c_f, the values of β, given in Table 1, show that in many cases Fr is considerably greater than unity unless w is a substantial fraction of $U \tan \beta$. To look at the dynamics of these fine-grained turbidity currents we may therefore need to use Equation 10 in its full form. The Chezy equation, which would suggest strongly supercritical flows, is probably inadequate.

We can estimate a number of the variables in Equation 10 (Table 1). From Equation 7 we have an estimate of τ, and using Equation 12 this can be interpreted as the flow velocity, U. The slope β is known approximately. The mean density of the flow ρ_t, can be expressed in terms of the total sediment concentration, N

$$\frac{\rho_t - \rho}{\rho_t} gh = \frac{\rho_s - \rho}{\rho_t} Ngh \simeq \frac{\rho_s - \rho}{\rho} Ngh \text{ as } \rho_t \simeq \rho \qquad (14)$$

where N and h remain to be determined. There are some, very broad, constraints on the values that can be assumed for these variables. Bagnold (1962) has suggested that for the flow to be fully turbulent, the Reynolds Number,

$$Re = \frac{Uh}{\mu} > 3000 \qquad (15)$$

where μ is the kinematic viscosity, Bagnold (1954) has also suggested that grain/grain interaction becomes dominant when,

$$N > 0{\cdot}09 \qquad (16)$$

The size ranges under discussion do not generally move as bedload. For suspended loads one expects the concentration to be relatively low, and to decrease as the current evolves downslope depositing the coarser silt and leaving the finer material behind.

Sediment dispersal and current thickness

McCave & Swift (1976) extended their idea of local deposition, leading to Equation 1, to consider the large scale dispersal pattern due to material being transported away from a source, where the concentration is C_0, under uniform flow conditions. Then, following Einstein (1968), the concentration at a distance x downstream is,

$$C=C_0 \exp\left[-w\left(1-\frac{\tau}{\tau_c}\right)p'\frac{x}{hU}\right] \qquad (17)$$

As the coarser material is deposited most rapidly, the concentration distribution becomes more and more weighted towards the finer material with distance downstream. Now, combining Equations 1 and 17 the deposition rate R,, becomes

$$R=\rho_s C_0 w\left(1-\frac{\tau}{\tau_c}\right)p' \exp\left[-w\left(1-\frac{\tau}{\tau_c}\right)p'\frac{x}{hU}\right] \qquad (18)$$

or,

$$\frac{R}{\rho_s C_0 p'}=\mathrm{f}(D) \exp\left[-X\mathrm{f}(D)\right] \qquad (19)$$

where

$$X=\frac{p'x,}{hU}$$

and

$$\mathrm{f}(D)=w\left[1-\frac{\tau}{\tau_c}\right]$$

is a known function of D for the silts. By differentiating Equation 19 it can easily be shown that the function, $\mathrm{f}(D) \exp\left[-X\mathrm{f}(D)\right]$, has a maximum value of $X^{-1}e^{-1}$ at $X\mathrm{f}(D_m)=1$, where D_m is the modal diameter of the deposited silt. Using this solution we have,

$$\frac{p'x}{hU}=\frac{1}{w\left(1-\frac{\tau}{\tau_c}\right)} \text{ for } D=D_{mode} \qquad (20)$$

x is the distance from the source, in this case the shelf break. Knowing x and using values of τ_c, w_s and U derived from D_m of a particular silt lamina, we can solve Equation 20 for h. Estimates of current thickness derived in this way are given in Table 1. They range from 580 to 1700 m (with three exceptions) assuming a value of $p'=1$. This gives a maximum thickness as p' cannot be greater than 1 and, presumably, may be significantly less than 1 for finer silt and mud which has more chance of escaping from the upper boundary layer. McCave & Swift (1976) use values of p' from 0·4 and 1·0. Using a value of $p'=0{\cdot}5$ we have thicknesses of 300–850 m.

These estimates of current thickness are of a comparable order of magnitude to the channel depths on the main fan, which range from 200 to 800 m; they are somewhat greater than those in the literature to date, Menard (1964) suggested that abyssal plain flows are a few tens of metres thick. However, Griggs & Kulm (1970) found evidence for Holocene turbidity currents in the Cascadia channel of about 120 m in thickness, and Komar (1977) points out that many deep sea fan channels with levees are up to 300 m deep.

The larger flows on the Laurentian Fan may be capable of topping the seamounts to the southwest of the Grand Banks, which Alam & Piper (1977) believed were out of reach of turbidity currents. The seamounts rise about 1000 m above the surrounding ocean floor and are covered, for the most part, by a slowly deposited, biogenic-rich, hemipelagic mud. However, there are certain intervals of fine, silt-laminated muds within the cores, which Alam & Piper supposed resulted from storm resuspension of material at the shelf break and transport along a density interface within the water column. They may in fact have been deposited from the upper part of thick, dilute turbidity currents, in which case they should be very fine grained, thinly laminated silty muds, perhaps equivalent to a more 'distal' (Sohm Abyssal Plain) turbidite sequence.

Time scales and current length

From Equation 8 we have,

$$\frac{Q}{C}=\frac{w(D)}{p_s(D)}\left(1-\frac{\tau}{\tau_c(D)}\right) \qquad (21)$$

where Q/C is a constant for any particular silt lamina estimated from the grain-size distribution (Fig. 7). Now, $C=p_b N_b$ where p_b is roughly constant (Fig. 4) and Q is defined by

$$Q=\frac{qN_s}{p'T_0}.$$

Thus the time T_0, for the deposition of any particular layer is,

$$T_0=\frac{qN_s}{p'p_b N_b}\left(\frac{Q}{C}\right)^{-1} \qquad (22)$$

We have data on N_s from porosity and water content measurements: it generally varies between 0·65 and

0·75. As discussed previously, p' probably lies between 0·4 and 1·0. Values of Q/C deduced from Equation 4 range from 0·1 for fine silts to 1·0 for coarse silts. These, together with laminae thicknesses, q, are shown in Table 1.

The least known quantity in Equation 22 is N_b, the concentration of the turbidity current. Bagnold (1962) suggests that the sediment concentration must be less than 0·09. Komar (1977) estimates the range of densities for turbidity currents at between 1·05 and 1·3 g cm^{-3}, which give concentrations spanning Bagnold's limit) however, these are for sandy, turbidity currents. Random measurements of suspended sediment concentrations in the nepheloid layer near the deep sea bed show values several orders of magnitude less than these values (0·01–0·54 mg l^{-1}, McCave & Swift, 1976, table 4).

A different estimate of N_b can be made by considering the volumes of slumps which may generate turbidity currents. We have, at any point x, slump volume − material already redeposited = total volume of current.

$$V_s - \int_0^x \frac{R}{\rho_s} dx = N_b LWh$$

so,

$$V_s > N_b LWh$$

where V_s is the slump volume and L, W and h are the length, width and thickness of the turbidity current. Various estimates of slump volumes are given in Table 2 (after Morgenstern, 1967); Komar (1969) suggests that the slump volumes for the larger Pleistocene turbidity currents in Monterey channel were of the order of 10^8–10^9 m^3.

A current thickness of 10^3 m, a width of 25 km (channel plus half levee widths) might be reasonable estimates. The length of the current is of the order of the mean velocity times the deposition time T_0.

Table 2. Volume of submarine slumps (after Morgenstern, 1967)

Location	Volume (m^3)
Magdalena River Delta	3×10^8
Mississippi River Delta	4×10^7
Suva, Fiji	$1{\cdot}5 \times 10^8$
Valdez, Alaska	$7{\cdot}5 \times 10^7$
Folla Fjord	3×10^5
Orkdals Fjord	10^7
Sagami Wan	7×10^{10}
Grand Banks Slope	10^8

$$L = UT_0 \qquad (22)$$

Then, following Komar (1969)

$$N_s V_s \simeq N_b WhUT_0 \qquad (23)$$

However, Equation 19 also provides a relationship between N_b and T_0 suggesting

$$N_b T_0 \sim 40 \text{ s}$$

then

$$N_s V_s \sim 10^8 \text{ m}^3 \qquad (24)$$

The present discussion has concentrated on the deposition of only fine-grained material, for this a contribution of the order of 10^8 m^3 seems of the right order. Although a value of $N_b T_0$ has been obtained this might represent deposition from fairly concentrated flow for a relatively short time or from a dilute suspension for a much longer time. Equation 22 has therefore been solved for T_0 for a range of concentrations from 10^{-4} to 10^{-2} (250–25,000 mg l^{-1}). The times taken for the deposition of individual silt laminae are given in Table 1. For $N_b = 10^{-3}$ (2500 mg l^{-1}), 5 mm of coarse silt or 1 mm of fine silt will be deposited in about 10 h.

Now, while the silt is depositing the mud concentration builds up to some critical value in the boundary layer, and then deposits very rapidly. It is therefore suggested that the silt deposition essentially determines the time scale for the whole unit, which is then given by integration of the depositional times of all silt laminae through a single unit. For 0·5 cm coarse silt and 0·5 cm fine silt (with perhaps 1–2 cm mud) we have a total deposition time of about 2·25 days. A thicker unit, say 2 cm silt and 4 cm mud, would take 4–6 days to deposit; or, for concentrations of 10^{-4} to 10^{-2} (250–25,000 mg l^{-1}) from a few hours to 1 or 2 months. It appears that concentrations of the order of 10^{-3} (2500 mg l^{-1}) give the most reasonable estimates of depositional times.

A single silt lamina would take several years to deposit from a flow with the concentration commonly reported from deep sea nepheloid layers (McCave & Swift, 1976; Pierce, 1976; Drake, 1976). The resulting deposit would be an homogeneous silty mud, without evidence of relatively rapid deposition and without distinct silt/mud lamination.

Current velocity and grain size

Several other points are evident from the data presented in Table 1. The current velocities deduced from deposition of the silt layers (coarse and fine) lie in a very close range of between 9 and 16 cm s^{-1}. This agrees well with the previous estimates of critical depositional velocities for fine-grained material (Einstein & Krone, 1962; Partheniades, 1964, 1965) and emphasizes the fact that clay will deposit rapidly from flowing water when it is sufficiently concentrated and flocculated.

From the discussion of Equation 13 it is clear that the characteristic settling velocity of the flow, $\bar{w}$, given by Equation 11 must be of the order of $U \tan \beta$. $\bar{w}$ cannot readily be estimated from the grain-size as it depends critically on the size distribution of the flocculated silt/mud suspension in the body of the turbidity current. However, the previous discussion has emphasized the possible relationship between grain and floc sizes suggested by various authors (particularly Kranck, 1973, 1975), as shown in Fig. 8. It was suggested that $w(D_f)$ for the mud is of the same order as $w(D_m)$ for the silt. The data in Table 1, and the relationship between $\bar{w}$ and $U \tan \beta$ (Fig. 11) reinforce this concept. The three anomalous points in Fig. 11 may be explained in various ways. One is from the upper slope and may represent part of a slump mass rather than a turbidity current deposit; another is from the distal end of the Laurentian fan and may be a particularly sandy layer from a suprafan channel. The third perhaps indicates the order of magnitude of the uncertainties involved in these various assumptions and calculations.

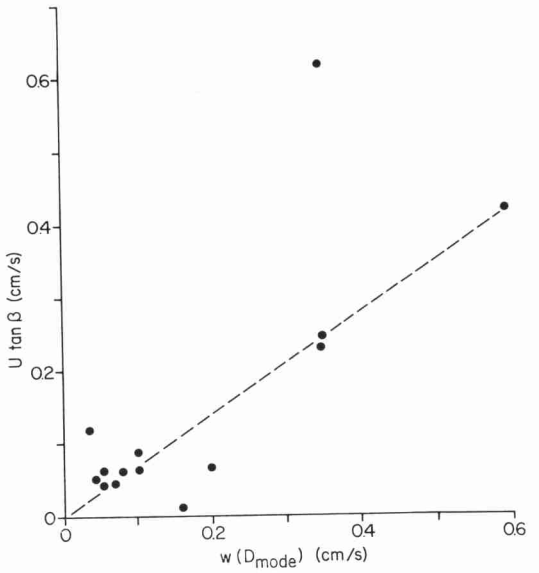

Fig. 11. $U \tan \beta$ versus w (mode), the characteristic settling velocity of the flow. The relationship shows the approximate equivalence of the two parameters as suggested in the discussion of Equation 10. The anomalously high and low values probably represent, respectively, samples from a muddy slump mass and a sandy suprafan channel.

CONCLUSIONS

A total picture of a turbidity current has been evolved in the previous discussion from the sedimentary characteristics of the silt-laminated muds on the outer Scotian margin. A new model is proposed for the origin of lamination by depositional sorting due to increased shear in the bottom boundary layer. This mechanism is consistent with previous work on fine-grained sediment dynamics, in particular, that of Kranck (1972, 1973, 1975) on floc properties; Krone (1962, 1963, 1972, 1976) on flocculation, deposition and shear destruction in the boundary layer; and others. The discussion of time scales has indicated how rapidly the sediment settles if the sediment dynamics up to the point where the mud is deflocculated in the boundary are determined primarily by the mode size of the silt.

The lateral, downslope evolution of sediment characteristics is consistent with the work of McCave (1970, 1972, 1976) and McCave & Swift (1976). The turbidity current model developed is consistent with the dynamic restraints discussed by Bagnold (1954, 1956, 1962), Ippen & Harleman (1952), Harleman (1961), and others. However, the overall system is significantly different from the picture commonly envisaged. The turbidity flows responsible for mud deposition on the outer Scotian margin are of a very large scale (up to 1000 m thick), of low concentration (about 10^{-3} or 2500 mg l^{-1}), and move downslope at velocities of 9–16 cm s^{-1}. Can such large, dilute slow flows still be considered turbidity currents? What evidence is there from other field measurements to support this concept?

There is in fact a growing body of observations that supports the proposed modification of the turbidity current theory but we have so far been slow to accept the changes implicit in these data. High velocities have only rarely been directly inferred for turbidity currents (e.g. the 1929 Grand Banks flow, Kuenen, 1952), although a competent current is clearly required for the transport of gravel down

deep sea canyons and channels. However, recent current-meter measurements in a variety of submarine canyons have all pointed to much lower velocity (50–150 cm s^{-1}) turbidity currents (Gennesseaux, Guibout & Lacombe, 1971; Shepard & Marshall, 1978, Keller & Shepard, 1978; Shepard *et al.*, 1977). Currents in fan valleys are usually slower than those in the canyons. Turbid layer underflows in lakes (Normark & Dickson, 1976; Lambert *et al.*, 1976) have demonstrated still lower velocities (maximum of 30 cm s^{-1}).

The levees and inter-channel areas of submarine fans are presumably constructed by turbidity current overflow of fan channels. The depth of those channels must therefore give some indication of flow thickness. Estimates from several tens (Menard, 1964) to several hundreds of metres (Griggs & Kulm, 1970; Komar, 1977) have been made, and channels on the Laurentian Fan are up to 800 m deep. Normark *et al.* (1980) have attempted to infer flow characteristics from the dimensions of sediment waves on the backsides of Monterey Fan Channel levees; they deduced a flow thickness of between 100 and 800 m.

Most estimates of flow concentrations have been for sandy turbidity currents (Komar, 1977) and these are one or two orders of magnitude greater than our 10^{-3} (2500 mg l^{-1}) figure. However, direct measurements of sediment concentration in canyon flows by Drake & Gorsline (1973) and Drake (1974) while Shepard and coworkers were measuring current velocities gave values of 2×10^{-7} to 2×10^{-6} (0·5–5 mg l^{-1}). These low-velocity, down-canyon surges have been attributed to storm build-up of shelf water against the coastline and to peak river discharge during floods. Shelf nepheloid layers have concentrations around 10^{-6} (2·5 mg l^{-1}) according to Pierce (1976). The average suspended-sediment concentration of the world's twenty major rivers (most of which result in large delta/fan complexes) is about 5×10^{-4} (1250 mg l^{-1}), and that of the next twenty is about 5×10^{-5} (125 mg l^{-1}) Strakov, 1967; Holeman, 1968). Actual concentrations during rainy seasons or times of flood may be considerably higher (Crickmay, 1974).

These several lines of evidence all support the concept of low-concentration, slow-moving, thick turbidity flows. We believe that these flows are important in carrying large quantities of fine-grained sediment to the deep-sea floor, both as separate sedimentation events and in association with the 'classical' higher-velocity, channelized turbidity currents.

ACKNOWLEDGMENTS

We thank Drs D. J. W. Piper and K. Kranck for many helpful discussions and their support in the laboratory analysis. Sediment samples were collected on Bedford Institute of Oceanography/Dalhousie University cruises over the past few years; and also from the Lamont–Doherty Geological Observatory core collection at Columbia University, New York; we would like to thank the many people involved. The Canadian Commonwealth Scholarship and Fellowship Committee provided support for D.A.V.S. which is gratefully acknowledged. The research was also supported by grants from Imperial Oil Ltd (Calgary) and the National Research Council (Canada) to D. J. W. Piper and A. J. Bowen. P. D. Komar and S. Smith are thanked for their valuable comments and critical review of the manuscript.

REFERENCES

ALAM, M. & PIPER, D.J.W. (1977) Pre-Wisconsin stratigraphy and palaeoclimates off Atlantic Canada, and its bearing on glaciation in Quebec. *Geogr. phys. Quat.* **31,** 15–22.

BAGNOLD, R.A. (1954) Experiments on gravity free dispersion of large solid spheres in a Newtonian fluid under stress. *Proc. R. Soc. Lond. A,* **225,** 49–63.

BAGNOLD, R.A. (1956) The flow of cohesionless grains in fluids. *Phil. Trans. R. Soc. A,* **249,** 235–297.

BAGNOLD, R.A. (1962) Auto suspension of transported sediments: turbidity currents. *Proc. R. Soc. Lond. A,* **265,** 315–319.

BULLER, A.J., GREEN, C.D. & MCMANUS, J. (1975) Dynamics and sedimentation: the Tay in comparison with other estuaries, In: *Nearshore Sediments, Dynamics and Sedimentation* (Ed. by J. Hails and A. Carr), pp. 201–250, John Wiley and Sons, London.

CRICKMAY, C.H. (1974) *The Work of the River.* Elsevier Publishing Co., New York.

DAILY, J.W. & HARLEMAN, D.R.F. (1966) *Fluid Dynamics.* Addison-Wesley Publishing Co. Inc., Massachusetts.

DAVIES, T.A. & LAUGHTON, A.S. (1972) Sedimentary processes in the North Atlantic, In: *Initial Reports of the Deep Sea Drilling Project,* Vol. XII (A. S. Laughton and W. A. Berggren *et al.*), pp. 905–934. U.S. Government Printing Office, Washington.

DRAKE, D.E. (1974) Distribution and transport of suspended solids in submarine canyons. In: *Suspended Solids in Sea Water* (Ed. by R. Gibbs), pp. 133–153. Plenum Press, New York.

DRAKE, D.E. (1976) Suspended sediment transport and deposition on continental shelves, In: *Marine Sediment Transport and Environmental Management* (Ed. by D. J. Stanley and D. J. P. Swift), pp. 127–158. John Wiley and Sons, New York.

DRAKE, D.E. & GORSLINE, D.S. (1973) Distribution and transport of suspended particulate matter in Hueneme,

Redondo, Newport and La Jolla submarine canyons, California. *Bull. geol. Soc. Am.* **84,** 3949–3968.

EINSELE, G., OVERBECK, R., SCHWARTZ, H.W. & UNSOLD, G. (1974) Mass physical properties, sliding and erodibility of experimentally deposited and differently consolidated clayey muds. *Sedimentology*, **21,** 339–372.

EINSTEIN, H.A. (1968) Deposition of suspended particles in a gravel bed. *Proc. Am. Soc. civ. Engrs J. hydraul. Div.* **94,** 1197–1205.

EINSTEIN, H.A. & KRONE, R.B. (1961) Estuarial sediment transport patterns. *Proc. Am. Soc. civ. Engrs, J. Hydraul. Div.* **67,** HY2, Part 1.

EINSTEIN, H.A. & KRONE, R.B. (1962) Experiments to determine modes of cohesive sediment transport in salt water. *J. geophys. Res.* **67,** 1451–1461.

EWING, M. & THORNDIKE, E.M. (1965) Suspended matter in deep ocean water. *Science,* **147,** 1291–1294.

EWING, M., EITTREIM, S.M., EWING, J.L. & LE PICHON, S. (1971) Sediment transport and distribution in the Argentine basin. In: *Physics and Chemistry of the Earth* (Ed. by L. H. Ahrens *et al.*), pp. 51–57. Pergamon Press, London.

GENNESSEAUX, M., GUIBOUT, P. & LACOMBE, H. (1971) Enregistrement de courants de turbidité dans la vallée sous-marine du var (Alpes-Maritimes). *C.r. hebd. Séanc. Acad. Sci., Paris,* **273,** 2456–2459.

GORSLINE, D.S., DRAKE, D.E. & BARNES, P.W. (1968) Holocene sedimentation in Tanner Basin, California continental borderland. *Bull. geol. Soc. Am.* **79,** 659–674.

GRIGGS, G.B. & KULM, L.D. (1970) Sedimentation in Cascadia deep sea channel. *Bull. geol. Soc. Am.* **81,** 1361–1384.

HARLEMAN, D.R.F. (1961) Stratified flow. In: *Handbook of Fluid Dynamics* (Ed. by V. L. Stretter). McGraw-Hill Book Co., New York.

HEEZEN, B.C., HOLLISTER, C.D. & RUDDIMAN, W.F. (1966) Shaping of the continental rise by deep geostrophic contour currents. *Science*, **152,** 502–508.

HESSE, R. (1975) Turbiditic and non-turbiditic mudstone of Cretaceous flysch sections of the eastern Alps and other basins. *Sedimentology,* **22,** 387–416.

HJULSTRØM, F. (1939) Transportation of detritus by moving water. In: *Recent Marine Sediments: A Symposium* (Ed. by P. D. Trask). *Spec. Publ. Soc. econ. Paleont. Miner., Tulsa*, **4,** 5–31.

HOLEMAN, J.N. (1968) The sediment yield of major rivers of the world. *Wat. Resour. Res.* **4,** 737–741.

HOLLISTER, C.D. (1967) *Sediment distribution and deep circulation in the western North Atlantic*. Unpublished Ph. D. Thesis, Columbia University.

IPPEN, A.T. & HARLEMAN, D.R.F. (1952) Steady state characteristics of sub-surface flow. *Natn. Bur. Stands Circ.* **521,** 79–93.

JOPLING, A.V. (1964) Laboratory study of sorting processes related to flow separation. *J. geophys. Res.* **69,** 3403–3418.

JOPLING, A.V. (1966) Some applications of theory and experiment to the study of bedding genesis. *Sedimentology*, **7,** 71–102.

JOPLING, A.V. (1967) Origin of laminae deposited by the movement of ripples along a stream bed: a laboratory study. *J. Geol.* **75,** 287–305.

KELLER, G.H. & SHEPARD, F.P. (1978) Currents and sedimentary processes in submarine canyons off the northeast United States. In: *Sedimentation in Submarine Canyons, Fans and Trenches* (Ed. by D. J. Stanley and G. Kelling), pp. 15–32. Dowden, Hutchinson and Ross, Stroudsburg, Pa.

KINGMA, J.T. (1958) The Tongaporutean sedimentation in central Hawke's Bay. *N.Z. J. Geol. Geophys.* **1,** 1–30.

KOMAR, P.D. (1969) The channelised flow of turbidity currents with application to Monterey deep-sea fan channel. *J. geophys. Res.* **74,** 4544–4558.

KOMAR, P.D. (1970) The competence of turbidity current flow. *Bull. geol. Soc. Am.* **81,** 1555–1562.

KOMAR, P.D. (1971) Hydraulic jumps in turbidity currents. *Bull. geol. Soc. Am.* **82,** 1477–1488.

KOMAR, P.D. (1973) Continuity of turbidity current flow and systematic variations in deep-sea channel morphology. *Bull. geol. Soc. Am.* **84,** 3329–3338.

KOMAR, P.D. (1977) Computer simulation of turbidity current flow and the study of deep-sea channel and fan sedimentation, In: *The Sea: Ideas & Observations on Progress in the Study of the Seas* (Ed. by E. D. Goldberg), pp. 603–621. John Wiley and Sons, New York.

KRANCK, K. (1972) Tidal current control of sediment distribution in Northumberland Strait, Maritime Provinces. *J. sedim. Petrol.* **42,** 596–601.

KRANCK, K. (1973) Flocculation of suspended sediment in the sea. *Nature*, **246,** 348–350.

KRANCK, K. (1975) Sediment deposition from flocculated suspensions. *Sedimentology*, **22,** 111–123.

KRONE, R.B. (1959) Silt transport studies utilising radioisotopes. *Second Ann. Rept, Inst. Engng Res., Univ. Calif., Berkeley.*

KRONE, R.B. (1962) Flume studies of the transport of sediment in esturial shoaling processes. *Hydraul. Engng Lab. Sanitary Engng Res. Lab., Univ. Calif., Berkeley,* 110 p.

KRONE, R.B. (1963) A study of rheological properties of estuarial sediments. *Hydraulic Engng Lab. Sanitary Engng Res. Lab., Univ. Calif., Berkeley*, 91 p.

KRONE, R.B. (1972) A field study of flocculation as a factor in estuarial shoaling process. *U.S. Army Corps Engrs Comm. Tidal Hydraul. Tech. Bull.* **19,** 62 p.

KRONE, R.B. (1976) Engineering interest in the benthic boundary layer. In: *The Benthic Boundary Layer* (Ed. by I. N. McCave), pp. 143–156. Plenum Press, New York.

KUENEN, PH. H. (1952) Estimated size of the Grand Banks turbidity current. *Am. J. Sci.* **250,** 874–884.

KUENEN, PH. H. (1966) Experimental turbidite lamination in a circular flume. *J. Geol.* **74,** 523–545.

LAMBERT, A.M., KELTS, K.R. & MARSHALL, N.F. (1976) Measurements of density underflows from Wallensee, Switzerland. *Sedimentology,* **23,** 87–105.

LAUGHTON, A.S., BERGGREN, W.A. *et al.* (1972) *Initial Reports of the Deep Sea Drilling Project*, Vol. XII. U.S. Government Printing Office, Washington.

LOMBARD, A. (1963) Laminites: a structure of flysh/type sediments. *J. sedim. Petrol.* **33,** 14–22.

MCCAVE, I.N. (1970) Deposition of fine grained suspended sediment from tidal currents. *J. geophys. Res.* **74,** 4151–4159.

McCave, I.N. (1972) Transport and escape of fine-grained sediment from shelf areas. In: *Shelf Sediment Transport: Process and Pattern* (Ed. by D. J. P. Swift, D. B. Duane and O. H. Pilkey), pp. 225–248. Dowden, Hutchison and Ross, Stroudsbrg, Pa.

McCave, I.N. (Ed.) (1976) *The Benthic Boundary Layer*, Plenum Press. New York.

McCave, I.N. & Swift, S.A. (1976) A physical model for the rate of deposition of fine-grained sediments in the deep sea. *Bull. geol. Soc. Am.* **87,** 541–546.

Menard, H.W. (1964) *Marine Geology of the Pacific*. McGraw-Hill, New York.

Migniot, C. (1968) Étude de propriétés physiques de différents sédiments très fins et de leur comportement sous des actions hydroynamiques. *La Houille Blanche*, **7,** 591–620.

Migniot, C. (1971) Utilisation de juages radioactives pour prévoir les conditions de tassement des sédiments fins ou mesurer la densité des sols dans les carottes de forage. *Laboratoire Central d'Hydraulique de France*, 5 pp.

Miller, M.C., McCave, I.N. & Komar, P.D. (1977) Threshold of sediment motion unidirectional currents. *Sedimentology*, **24,** 507–528.

Moon, C.F. (1972) The microstructure of clay sediments. *Earth Sci. Rev.* **8,** 303–321.

Moore, D.G. (1969) Reflection profiling studies of the California Continental borderland: Structure and Quaternary turbidite basins. *Spec. Pap. geol. Soc. Am.* **107,** 142p.

Morgenstern, N.R. (1967) Submarine slumping and the initiation of turbidity currents. In: *Marine Géotechnique* (Ed. by A. F. Richards), pp. 189–220. University of Illinois Press, Urbana, Ill.

Normark, W.R. & Dickson, F.H. (1976) Sublacustrine fan morphology in Lake Superior. *Bull. Am. Ass. Petrol. Geol.* **60,** 1021–1036.

Normark, W.R., Hess, G.R., Stow, D.A.V. & Bowen, A.J. (1980) Sediment waves on the Monterey Fan levee: a preliminary physical interpretation. *Mar. Geol.* (In press.)

Odd, N.W.M. & Owen, M.W. (1972) A two-layer model for mud transport in the Thames estuary. *Proc. Inst. civ. Engrs Lond., Suppl.* (ix) paper 7517S.

Partheniades, E. (1964) A summary of the present knowledge of the behaviour of fine sediments in estuaries. *School of Engng Mass. Inst. Tech., Hydrodynamics Lab., Tech. Note,* **8,** 47p.

Partheniades, E. (1965) Erosion and deposition of cohesive soils. *Proc. Am. Soc. civil Engrs, J. hydraul. Div.* **91,** HY1, 106–139.

Partheniades, E. & Paaswell, R.E. (1968) Erosion of cohesive soil and channel stabilization. *Civ. Engng Rep.* **19,** State University of New York, Buffalo.

Partheniades, E., Cross, R.H. & Ayora, A. (1969) Further results on the deposition of cohesive sediments. *Proc. 11th Conf. Coastal Engng, London*, 1968, pp. 723–742.

Pierce, J.W. (1976) Suspended sediment transport at the Shelfbreak and over the outer margin. In: *Marine Sediment Transport and Environmental Management* (Ed. by D. J. Stanley and D. J. P. Swift), pp. 437–458. John Wiley and Sons, New York.

Piper, D. J. W. (1972) Turbidite origin of some laminated mudstones. *Geol. Mag.* **109,** 115–126.

Piper, D.J.W. (1975) Late Quaternary deep water sedimentation off Nova Scotia and the western Grand Banks. *Mem. Can. Soc. Petrol. Geol.* **4,** 195–204.

Piper, D.J.W. (1978) Turbidite muds and silts on deep sea fans and abyssal plains. In: *Sedimentation in Submarine Canyons, Fans and Trenches* (Ed. by D. J. Stanley and G. Kelling), pp. 163–176. Dowden, Hutchinson and Ross, Stroudsburg, Pa.

Sanders, J.E. (1960) Origin of convoluted laminae. *Geol. Mag.* **97,** 409–421.

Sanders, J.E. (1965) Primary sedimentary structures formed by turbidity currents and related sedimentation mechanisms. *Spec. Publ. Soc. econ. Paleont. Miner., Tulsa,* **12,** 192–265.

Sheldon, R.W. & Parsons, T.R. (1967) *A Practical Manual on the Use of the Coulter Counter in Marine Science*. Coulter Counter Electronics Inc., Toronto, 66p.

Shepard, F.P. & Marshall, N.F. (1978) Currents in submarine canyons and other sea valleys. In: *Sedimentation in Submarine Canyons, Fans and Trenches* (Ed. by D. J. Stanley and G. Kelling), pp. 11–14. Dowden, Hutchinson and Ross, Stroudsburg. Pa.

Shepard, F.P., McLoughlin, P.A., Marshall, N.F. & Sullivan, G.G. (1977) Current meter recordings of low-speed turbidity currents. *Geology*, **5,** 297–301.

Stow, D.A.V. (1975) *The Laurentian Fan – Late Quaternary Stratigraphy*. Unpublished Report, Dalhousie University, Halifax, Canada. 81p.

Stow, D.A.V. (1976) Deep water sands and silts on the Nova Scotian Continental margin. *Mar. Sedim.* **12,** 81–90.

Stow, D.A.V. (1977) *Late Quaternary stratigraphy and sedimentation on the Nova Scotian Outer continental margin*. Unpublished PhD Thesis, Dalhousie University, Halifax, Canada. 361p.

Stow, D.A.V. (1979) Distinguishing between fine-grained turbidities and contourites on the deep-water margin off Nova Scotia. *Sedimentology*, **26,** 371–387.

Stow, D.A.V. & Bowen, A.J. (1978). Origin of lamination in deep-sea, fine-grained sediments. *Nature*, **274,** 324–328.

Strakov, N.M. (1967) *Principles of Lithogenesis*, Vol. 1, Consultants Bureau, New York.

White, S.J. (1970) Plane bed thresholds of fine-grained sediments. *Nature*, **228,** 152–153.

Whitehouse, U.G., Jeffrey, L.M. & Debbrecht, J.D. (1960) Differential settling tendencies of clay minerals in saline waters. In: *Clay and Clay Minerals* (Ed. by A. Swineford), pp. 1–79. Pergamon Press, Oxford.

Wood, A. & Smith, A.J. (1959) The sedimentation and sedimentary history of the Aberystwyth Grits. *Q. J. geol. Soc. Lond.* **94,** 163–190.

Young, R.A. & Southard, J.B. (1978) Erosion of fine-grained marine sediments: sea floor and laboratory experiments. *Bull. geol. Soc. Am.* **89,** 663–672.

(*Manuscript received* 17 *May* 1978; *revision received* 15 *February* 1979)